INFLUENCE OF TRANSPORT PHENOMENA ON THE STRUCTURE OF LEAN PREMIXED HYDROGEN AIR FLAMES

Nikolai Ardey
Lehrstuhl A für Thermodynamik
Technische Universität München
80290 Munich, Germany
+49 - 89 - 2105 3458

Franz Mayinger
Lehrstuhl A für Thermodynamik
Technische Universität München
80290 Munich, Germany
+49 - 89 - 2105 3436

Bodo Durst
Lehrstuhl A für Thermodynamik
Technische Universität München
80290 Munich, Germany
+49 - 89 - 2105 5174

ABSTRACT

Due to the release of hydrogen during a hypothetical severe accident in a light water reactor, intense efforts are made on the investigation of premixed hydrogen-air-combustion and connected safety aspects. Hydrogen combustion in the course of a gradual hydrogen release normally starts out from slow deflagrations, which, however, can be accelerated to very high flame speeds by flame-obstacle-interaction yielding a complex superimposition of chemical kinetics and turbulent heat and mass transfer. The influence of molecular transport phenomena on undisturbed flame propagation and turbulent flame acceleration processes caused by flow obstacles with high blockage ratios are demonstrated by explosion tube experiments applying laser-optical flame diagnostics. Mainly two effects have been identified. Flame instability in the lean regime of hydrogen combustion enhances the sensitivity for turbulent flame acceleration due to low Lewis number effects. In the vicinity of highly blocking obstacles partial quenching is achieved by rather high turbulence leaving unburned radicals, which form a highly reactive mixture in the jetflow behind the obstacle.

I. INTRODUCTION

Previous and recent work on obstacle induced flame acceleration has been performed in explosion tubes of different scales by a number of researchers [9], [19], [21], [24] using orifices and baffles with different blockage ratios *BR*. Flame acceleration has been detected by equally spaced photodiodes or highspeed thermocouples along the tube axis measuring the integral flame speed. In order to correlate the obtained flame speeds with turbulent flow characteristics for modeling purposes, LDV- and hot wire measurements were used for flow diagnostics ([18], [24], i.a.). Different modes of combustion could be derived from those correlations, classified by a number of ratios and could be summarized in a phase diagram, which appeared to be a valuable tool for the general assessment of combustion processes in any turbulence regime, by Borghi [5] (see fig. 1) and Peters [20].

$$\text{Damköhler number } Da = \frac{\tau_L}{\tau_c}$$

$$\text{Karlovitz number } Ka = \frac{\tau_c}{\tau_K} \qquad (1)$$

$$\text{turb. Re number } Re_L = \frac{u' L}{\nu}$$

A comprehensive discussion of the different combustion regimes is to be found in [20]. Within the flamelet regime flame fronts are generally envisaged as thin, continuous and locally laminar reaction zones completely separating burnt and unburned gases to be properly described by fast chemistry approaches. Flame acceleration is achieved in this regime by surface enlargement due to flow strain causing flame stretching. Beyond the limit of $Ka=1$ flame stretch causes partial quenching and reaction zones are thickened due to the entrainment of Kolmogorov-small scale vorticity yielding maximum strain rates (distributed reaction zones). Abdel Gayed et al. found a quenching criterion within the regime of distributed reaction zones, given by the product of the Karlovitz flame stretch factor K and the Lewis number Le:

$$K\,Le = 1.5;\ K = \frac{u'}{s_l}\frac{\delta_l}{\lambda_T};\ Le = \frac{a}{D} \qquad (2),$$

stating that flame surface enlargement predominates the reduction of local chemical reaction rates by turbulent quenching below that limit and the other way around. Hence, flame speeds reach a maximum value at the limit of $K\,Le = 1.5$ [18]. The present paper takes advantage of the aforementioned criteria in order to characterize the burning conditions obtained from experiments and takes not any efforts to further improve the general

understanding of the impact of flow strain on the integral burning rate, which is to be applied in an averaged manner over the locally complex shaped flame front.

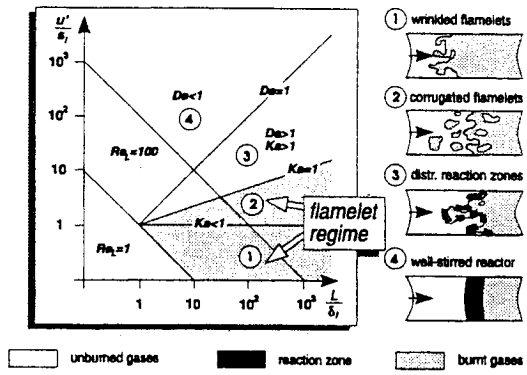

Fig. 1: Phase diagram for turbulent premixed combustion according to Borghi [5]

Lack of experimental consistency in connection with flow obstacles [9], facility-specific phenomena not sufficiently identified and considerable data scattering [e.g. 14], lead to the request for deeper insights to the physics of turbulence-chemistry-interaction in general, to gain margin in the transferability to containment typical conditions. Highspeed schlieren photographs and stroboscopic flame records, which were performed to qualitatively visualize the leading flame contour [6], [12], [24], [25], substantially improved the understanding of flame propagation in a turbulent flow field. However, due to the limits of spatial resolution in depth, schlieren photographs can not resolve the structure of strongly convoluted flames appearing in the vicinity of obstacles.

To get around that problem, laser-light-sheet methods have been developed taking advantage of fluorescence and scattering properties of process involved molecules or added tracer particles and molecules. The majority of related work applying those methods for hydrogen-air combustion focuses on steady atmospheric flames. Goix and Shepherd [8] used a stagnation point flame burner and visualized the flame contour by means of Mie-scattering of silicon oil droplets evaporating in the burnt region. They observed a significant dependence of the flame surface area on the ratio of thermal diffusivity a of the mixture and mass diffusivity D of the species deficient (H_2 in the lean case), which is characterized by the Lewis number

$$Le = a/D. \qquad (3)$$

It was concluded that flames behave unstable with low Le numbers maximizing their surface area and the other way around. The evaluation of flame curvature pdf's resulted in more or less symmetric curvature distributions with a slight bias towards positive curvatures with low Le numbers. Applying a planar OH-Laser Induced Fluorescence technique (OH-LIF) on the investigation of steady V-shaped flames interacting with shedded Karman vortices, Lee et al. [15] revealed both the leading flame contour and the local reactivity providing quantitative evaluation of chemical aspects connected to flame surface properties with respect to molecular and turbulent transport.

Due to Taylor-Markstein-instabilities [17], generated by density- and pressure discontinuities along the flame front, additional phenomena have to be taken into account with freely propagating flame fronts in a confined volume interacting with self induced expansion flow. Detailed flame structure analyses of unsteady propagating flames based on OH-LIF-data is almost solely available for hydrocarbon flames [7], [16], [23]. Efforts on the visualization of the structure and local reactivity of H_2-air flame fronts propagating around an obstacle are presently not known.

The present work, therefore, was aimed at phenomenological analyses of disturbed and undisturbed propagation of premixed H_2-air flames applying a planar OH-LIF technique in order to identify mechanisms of flame acceleration which are not yet satisfactorily understood.

II. EXPERIMENTAL APPARATUS

A small scale facility has been used to investigate unsteady propagating flame fronts consisting of a pulsed flame generator with a rectangular cross section of 26×60 mm (fig. 2), which was connected to a H_2-air mixing and supply system. Quartz windows provided proper optical access for LIF-imaging. Within the window section a flow obstacle could be applied. To vary the rms fluctuating velocity u', a steady flow of H_2-air mixtures was superimposed to the flame propagation. Single flame fronts traveling in the mean flow direction were generated by spark igniters. The unburned mixture escaping the tube was trapped by a pilot flame. An exit nozzle prevented the pilot flame from lifting off and entering the tube against the flow direction.

The laser optical set-up was composed of a XeCl EXCIMER-laser emitting 17 ns laser pulses at 308 nm and an arrangement of cylindrical and spherical lenses and mirrors to form a laser light sheet with a thickness of about 0.3 mm and a height of 45 mm (fig. 3).

Within the laser light sheet the (0,0)-band of the $A^2\Sigma \rightarrow X^2\Pi$ system of the OH-radicals is electronically excited with a relaxation time of about 10^{-8} to 10^{-6} s. Returning to their original quantum state the OH-radicals emit fluorescence light without a wave length shift to the excitation light. The fluorescence signal has been observed perpendicularly to the laser incident beam with a UV-intensified CCD-camera. The obtained gray scale images

were evaluated and transformed to pseudo color images by a digital image processor. Due to the short laser pulse duration chemically frozen images were obtained displaying the longitudinal section of the propagating flame fronts.

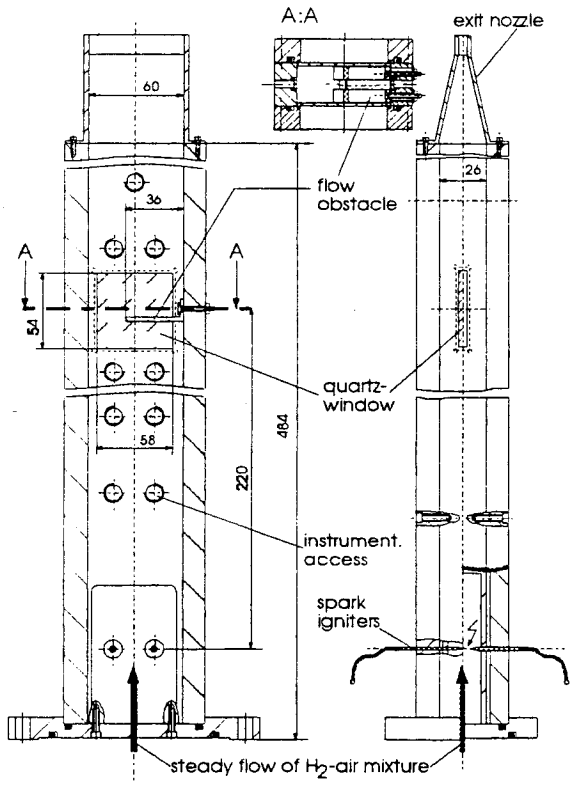

Fig. 2: Pulsed flame generator for unsteady flame propagation analysis

As a major species rising during the chemical reaction of H_2 and O_2 the OH-radicals indicate the location and spread of the reaction zones. The number density of OH-molecules in the reaction zone correlates with the local reaction rate of H_2 and O_2 and is measured by the intensity of the OH-LIF signal ER_{LIF}, which is a linear function of the number density N [19]:

$$ER_{LIF} = N\, E_1\, B_{12}\, I_{\nu,L}\, \frac{A_{21}}{A_{21} + Q_{21}} \qquad (4)$$

Whilst the population of the ground state E_1, the Einstein coefficient B_{12} and the quantum transfer coefficients A_{21} can be either calculated or picked out from tables, the quenching coefficient Q_{21} is unknown. Hence, only relative distributions of the local reaction rate are to be deduced from LIF-images. Further uncertainty is obtained from the spectral laser intensity $I_{\nu,L}$, which varies over a range of about 10%.

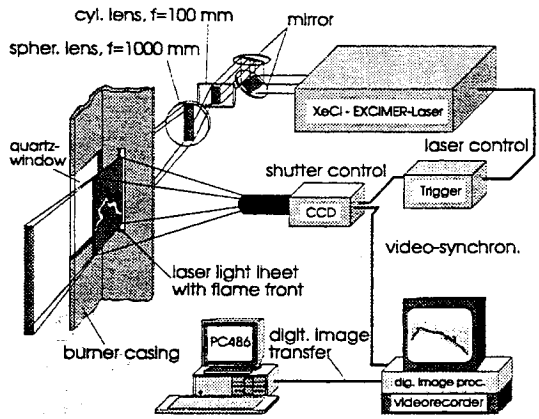

Fig. 3: Optical set-up for OH-LIF imaging

III. EXPERIMENTAL CONDITIONS

In order to cover the relevant conditions for accidental combustion scenarios in LWR's, H_2-concentrations in the lean regime of 9 to 16.5 vol.% in air and corresponding equivalence ratios of ϕ=0.24 to 0.47 have been investigated. The thermo-fluid dynamic mixture properties are summarized in tab. 1.

γ_{H2} vol.%	mixture properties at 293 K			
	ν 10^{-5} m²/s	λ 10^{-1} W/mK	ρ Kg/m³	a 10^{-5} m²/s
9,0	1,565	0,31	1,09	2,59
11,5	1,605	0,32	1,06	2,68
13,0	1,625	0,33	1,045	2,76
16,5	1,673	0,36	1,01	3,00

Tab. 1: Thermo-fluid dynamic mixture properties

Laminar flame speed data from Koroll et al. [10] were used to determine the laminar burning conditions shown in tab. 2. For the laminar flame thickness Abdel Gayed et al. [2] give a simple relationship under the assumption of a uniform Prandtl number:

$$\delta_l = \nu / s_l\,, \quad \text{with} \quad Pr = \nu / a = 1 \qquad (5)$$

The chemical time scales are then determined by

$$\tau_c = \delta_l / s_l \qquad (6)$$

γ_{H2} vol.%	s_l m/s	τ_c µs	δ_l µm
9,0	0,19	432	82
11,5	0,31	168	52
13,0	0,48	71	34
16,5	0,92	20	18

Tab. 2: Laminar burning conditions

As turbulence intensities of tube flows can be taken to be nearly constant with Re numbers not changing over orders of magnitude, the absolute value of the rms fluctuating velocity u' has been varied by superimposing a

steady flow of 5÷20 m/s to the flame propagation, yielding *Re* numbers of 11,250 to 45,000.

IV. RESULTS AND DISCUSSION

A. Investigation of undisturbed flame propagation

The influence of flow obstacles with low blockage ratios (*BR*<15%) is generally characterized by a more or less homogeneous enhancement of turbulence intensity without the effects of fully shedded boundary layers and jet formation [19]. To simulate those phenomena and to gain an understanding of freely propagating flame fronts before they pass a highly blocking obstacle, experiments have been performed without any obstacle. Turbulence intensities generated by the superimposed steady flow have to be expected in the range of 6÷8% for the given regime of *Re* numbers due to Laufer [13]. Flame propagation in the mean direction of a superimposed steady flow can be treated like flame propagation in a tube, vented at both ends. Heat released by combustion is transferred to the continuously flowing fresh gases. Hence, flame generated flow is suppressed to a great extent and the superimposed steady flow can be considered as turbulent flow conditions right ahead of the flame in a first approach. Taking into account the laminar burning conditions (tab. 2) a phase diagram for turbulent combustion modes has been drawn for lean hydrogen mixtures (fig. 4) with respect to the combustion regimes, marked off by Borghi (fig. 1). The quenching limit of $K\,Le$=1.5 has been derived from a relation, which was given for the flame stretch factor K by Abdel Gayed et al. [3] under consideration of converting formulas between different length scales to be found in [1]:

$$K = 0.157\left(\frac{u'}{s_l}\right)^2 Re_L^{-0.5} \qquad (7)$$

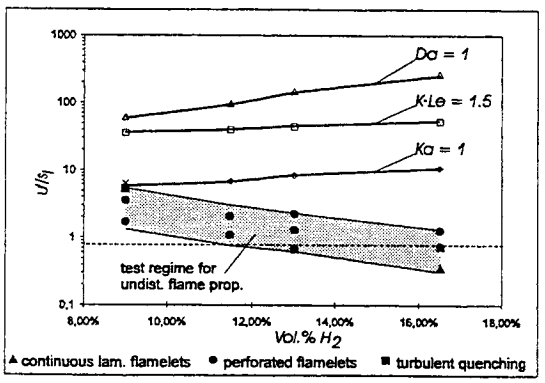

Fig. 4: Phase diagram for lean H_2-air flames and observed flame structure characteristics

As shown in fig. 4, the turbulent burning conditions within the present experiments cover the flamelet regime and remain clearly below the limit of *Ka=1*, except the very lean mixture with a content of 9 vol.% H_2.

Fig. 5 shows exemplarily the typical appearance of OH-LIF-images obtained from the present experiments. The darker the local gray scale the higher the number density of OH-radicals observed. A gray background in the unburned regime originates from light reflections and elastic Rayleigh scattering processes, which disappear in the burnt regime due to a decreasing density. With respect to the low scattering cross section of the Rayleigh scattering process in comparison to the Laser induced Fluorescence, the LIF-signal normally stands out clearly against the Rayleigh signal.

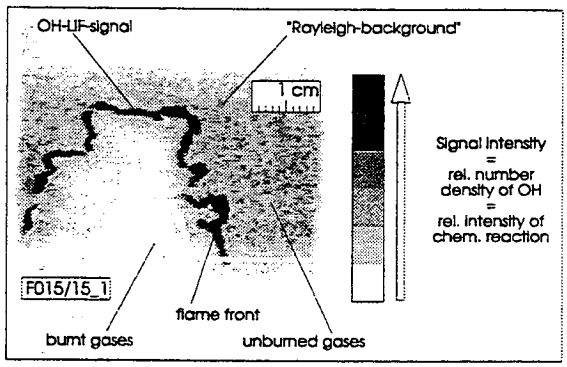

Fig. 5: Typical OH-LIF image of a propagating flame front

A representative selection of obtained LIF-images is arranged in fig. 6 in a certain order according to the flow velocity and the H_2-concentration. It can obviously be distinguished between thin and locally laminar flamelets and distributed reaction zones exceeding the limit of *Ka=1* which only happened to the mixture of 9 vol.% H_2 at 15 m/s, as expected. But the flamelets surprisingly show clear interruptions against the common idea of continuous flamelets completely separating burnt and unburned gases by thin reaction zones.

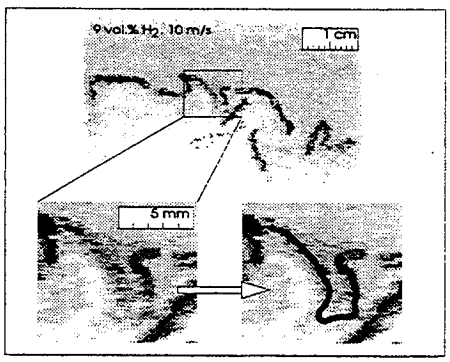

Fig. 7: Continuous completion of an apparent quenched flame section

The interruptions are partially caused by OH-LIF-signals dropping down beneath the detection limit. In this case the flame contour may be completed to a continuous curve as demonstrated in fig. 7.

A lot of further interruptions of the flame contour are not to be continuously completed and show obvious quenching (fig. 8).

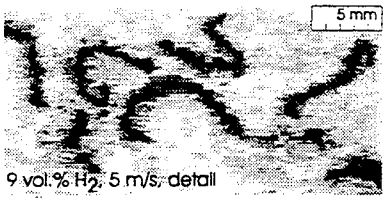

Fig. 8: Example for obvious quenching effects within the flamelet regime

Continuous flamelets without any interruptions have only been observed below the limit of $u'/s_l=1$. A survey on the obtained flame structure characteristics according to the ratio of u'/s_l and the H_2-concentration is given in the phase diagram of fig. 4.

Since flame front perforation due to turbulent flow strain is not to be expected within the flamelet regime, the reason for that behavior must be derived from molecular transport phenomena right ahead of the flame. Surface enlargement due to positive curvature enhancement towards the unburned mixture leads to larger preheating zones with increasing heat losses of the reaction zone by thermal diffusion, which would damp the chemical reaction rate. On the other hand, enlarged preheating zones contain more molecules of the deficient reaction partner (H_2 in the lean case) to be transported into the reaction zones by mass diffusion (fig. 9).

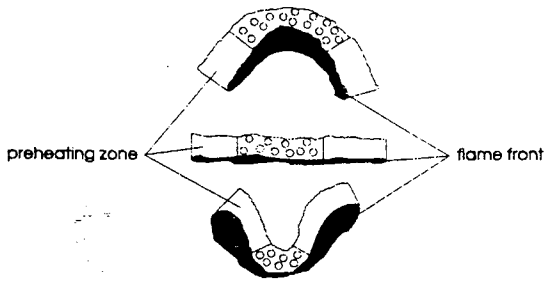

Fig. 9: The effect of flame curvature on the apparent H_2-concentration in the preheating zone

Within the regime of lean H_2-air combustion the latter effect predominates the effect of thermal diffusion because of a rather high mass diffusivity of H_2 in air compared to the thermal diffusivity of H_2-air mixtures, which becomes apparent in considerably low *Le* numbers (3). I.e. even small excursions of the flame contour by vortex-flame interaction trigger the flame to increase its curvature towards the unburned mixture in order to maximize the chemical conversion rate. Gaining maximum reactivity at positive curved flame sections the flame front is inevitably quenched by even small flow disturbances at the complementary appearing negative curved sections (fig. 6). This mechanism, which is referred to as diffusive flame instability, leads to an increase of flame surface area in addition to flame stretching by turbulent flow strain.

Decreasing *Le* numbers and an increasing impact of the *Le* number on mass diffusion of the deficient reactant with decreasing H_2-concentrations (fig. 10) cause lean flames to be more unstable than rich ones resulting in larger flame

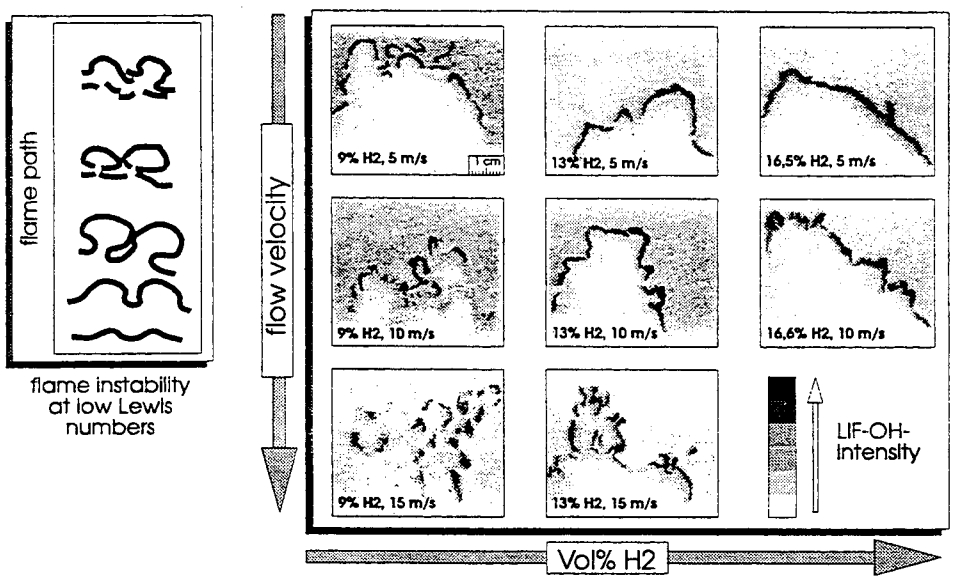

Fig. 6: OH-LIF-images of freely propagating flame fronts

surface areas at the same turbulence intensity (fig. 6, 11). Hence, sensibility to turbulent flame acceleration increases with decreasing hydrogen concentrations within the flamelet regime.

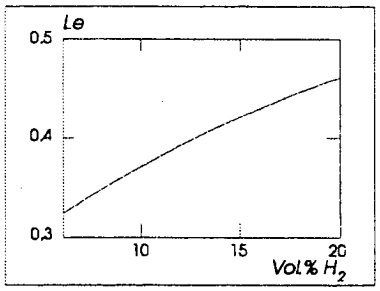

Fig. 10: Le number of H_2-air mixtures at ambient temperature applying the binary mass diffusivity of H_2 in N_2 and considering the preheating zone of H_2-air flames to be almost inert.

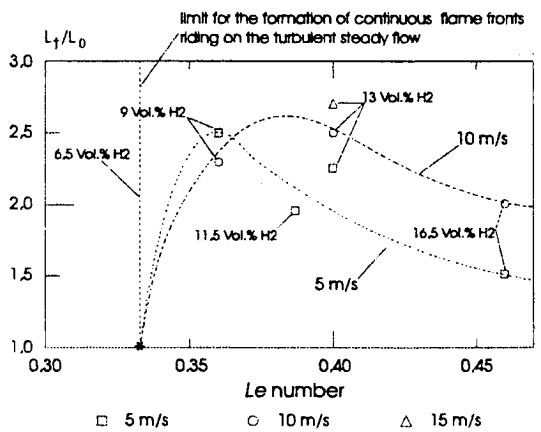

Fig. 11: Effect of the Lewis number on the flame perimeter

Assuming the enhanced reactivity at positive curved flame sections to be in balance with weakened reactivity at negative curved sections it can be concluded in a first order approach that turbulent burning rates are sufficiently expressed by the product of flame surface enlargement ratio A_F/A_0 and the laminar flame speed within the flamelet regime (8), although the flamelets are perforated.

$$s_t = \frac{A_F}{A_0} s_l \qquad (8)$$

The turbulent burning speeds, which were derived from the square of the flame perimeters, related to their normal projection in order to approach the ratio of A_F/A_0, are displayed in fig. 12. A comparison with turbulent burning speeds, established by Abdel Gayed et al. [2] at similar conditions concerning K and Re_L, shows rather good agreement. Considerable data scattering is obtained which may be reduced if the flame perimeter would be weighted with local reactivities, not quanti-tatively evaluated in the present work. However, the turbulent burning speed matches in fig. 12 tendentiously exhibit the aforementioned increasing sensitivity to turbulent flame acceleration with decreasing H_2-concentrations.

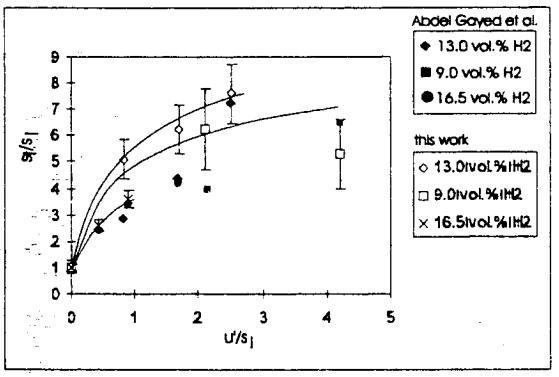

Fig. 12: Turbulent burning speeds as a function of the rms fluct. vel. u', derived from flame perimeters and corresponding data from Abdel Gayed et al. [2]

The presented evaluation methods for OH-LIF-images in order to characterize flame surface properties in detail, is only valid for discrete, partially continuous and thin flamelets. For locally quenched distributed reaction zones, the area covered by the diffuse reacting shreds (fig. 6, 9 vol.% H_2, 15 m/s) related to the whole spread area of the flame taken from the 2D-LIF-imagas may be a proper criterion.

B. Flame fronts interacting with a baffle

Further flame acceleration to violent combustion modes is only possible beyond the flamelet regime if the limit of $KLe=1.5$ for flame deceleration by strong turbulent quenching is not exceeded. However, *partial* turbulent quenching is closely linked to strong flame acceleration. Turbulence intensities that are high enough to cause turbulent quenching, occur most likely in highly turbulent shear layers, separating at the edges of highly blocking obstacles. To demonstrate this effect, OH-LIF-images were taken of flame fronts passing a plate shaped obstacle with a blockage ratio BR of about 60% (fig. 13a, 13b). Again a steady flow of 5 to 15 m/s was superimposed to the flame propagation in order to vary the rms fluctuation velocity u'. Phylaktou et al. [21] specified the obstacle induced turbulence intensities in the shedded shear layer behind baffles of BR=60% to reach values of about 0.6. The burning conditions exceeding the flamelet limit of $Ka=1$ based on the least values for u' according to the steady flow are shown in fig. 14. Additional fluctuations due to flame induced expansion flow which does not appear to be negligible in blocked flows, have to be taken into account.

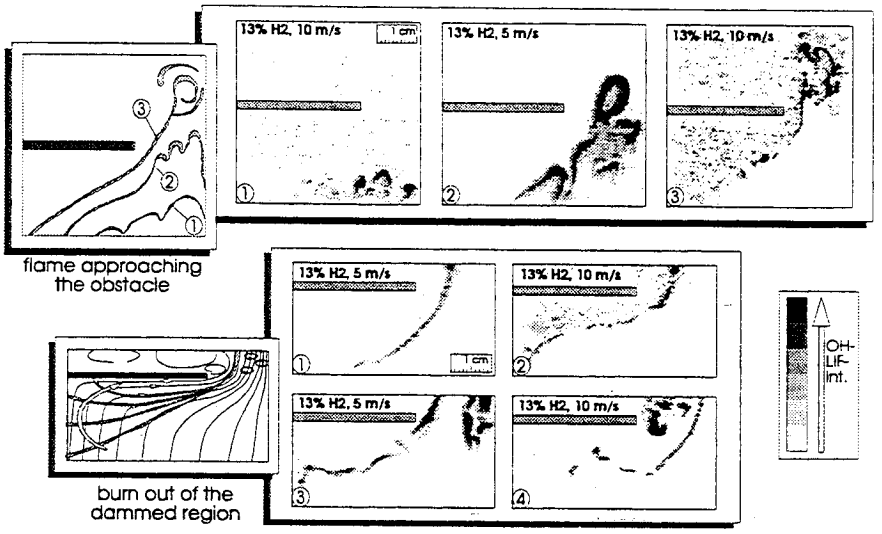

Fig. 13a: OH-LIF images of H_2-air flames passing a baffle with BR=60%

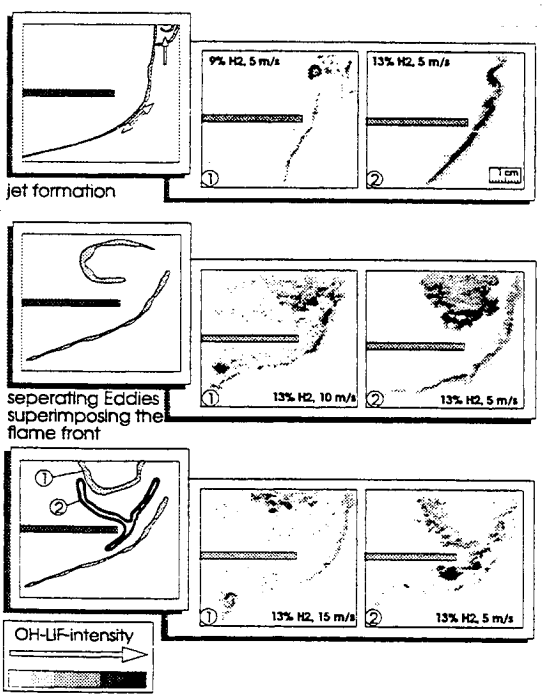

Fig. 13b: OH-LIF images of H_2-air flames passing a baffle with BR=60%

Although only single shot images were obtained for the flame fronts passing the obstacle, the development of the flame structure could be reconstructed evaluating quite a number of single shots representing different time steps of the event.

Following the flow contraction in front of the obstacle the flame front appears intensely corrugated in comparison to the undisturbed flame shape. The main part of the flame front moves ahead of the obstacle riding on the contracted jet flow (fig. 13b, 1st. row), whilst a considerably smooth flame contour in front of the obstacle remains a certain time until the blocked area is burnt. The flame contour is, thereby, exposed to a counter flow and determined by the locations where the flow component normal to the flame front is equal to the local burning speed or less (fig. 13a). When the flame front entrains the back-flow zone penetrating the shear layer it is superimposed to the vortices separating at the edge of the obstacle (fig. 13b, 2nd. row). The flame front is partially carried with the vortices, if the vortex propagation velocity exceeds the local burning velocity. Quite a number of images exhibited flame fronts "escaping" the vortex and burning back into the unburned dammed area in the case of a lower vortex propagation velocity (fig. 13b, 3rd. row).

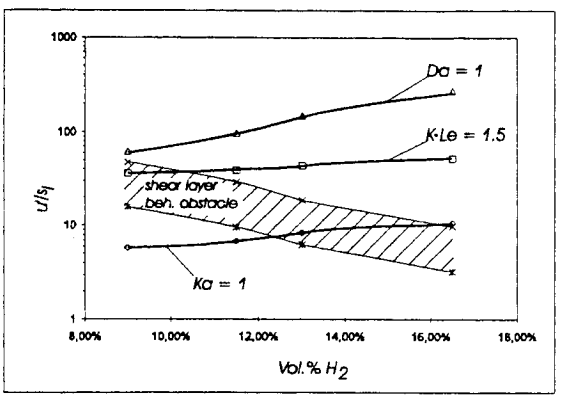

Fig. 14: Burning conditions behind the obstacle, based on the least values for u' in the shear layer

Considerably strong quenching of flame parts in the vicinity of the separation edge has been observed, caused by high turbulence intensities as expected from the presupposed burning conditions (fig. 14). Unburned radicals originating from aborted chemical reactions are

"washed out" from the shredded reaction zones and transported ahead of the flame by the accelerated jet flow showing high velocity-components tangential to the leading flame contour. Hence, the flame propagation is strongly disturbed and even decelerated right in the vicinity of the obstacle, which has also been observed from own experiments in an explosion tube of larger scale (0.268×0.268×3 m) applying a plate shaped obstacle with a blockage ratio of 85%, where the integral flame speed was measured with UV-sensitive photodiodes (fig. 15).

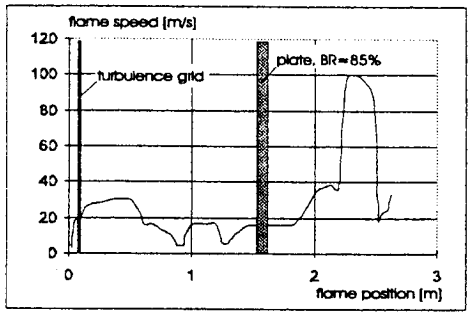

Fig. 15: Flame speed along an explosion tube with a cross section of 268×268 mm and a plate shaped obstacle (BR=85%) at 1.6m behind ignition, initially filled with a mixture of 12 vol.% H_2 in air

When the partially quenched flame front reforms at a certain distance behind the obstacle, where the turbulent flow strain is decayed, it becomes much more wrinkled and convoluted than it was before the obstacle due to the distribution of the small reacting shreds. Running into the region, which is enriched by unburned radicals originating from highly turbulent quenching zones, the flame becomes strongly accelerated. In DDT-sensitive mixtures local explosions are likely to occur in the radical-enriched zones, which amplify themselves to detonation waves. The latter mechanism is generally referred to as "hot jet ignition". However, turbulent quenching is closely linked to severe flame acceleration and DDT as a triggering mechanism.

V. CONCLUSIONS:

A phenomenological analyses of disturbed and undisturbed flame propagation in lean H_2-air mixtures has been presented, based on small scale explosion tube experiments and planar OH-LIF images of the flame structure at various rms fluctuation velocities.

The burning conditions for undisturbed flame propagation were almost confined within the flamelet regime with respect to the experimental flow conditions. An increasing bias of the flame curvature distribution towards positive values with a decreasing equivalence ratio and maximum reactivities at positive curved sections against local quenching at negative curved sections has been observed, pointing at flame instability due molecular transport effects. The considerably hi diffusivity of hydrogen in air $D_{H2/air}$ in comparison to t thermal diffusivity a, characterized by low Lewis numbe ($Le=a/D$) causes the flame front to preferentially increa the flame surface and preheating zone by positiv curvature enhancement. Hence, the flame front inevitabl severs at negative curved sections showing less reactivit and high quenching sensitivity to flow strain. Since th significance of flame instability increases due to a Lewi number decay with decreasing hydrogen concentrations lean flames are more sensitive to turbulent flam acceleration than rich ones.

A plate shaped obstacle with BR=60% has been applied to representatively demonstrate the mechanisms of flame-obstacle interaction at high blockage ratios. Beside the effect of flame acceleration by jet-formation and significant surface enlargement due to vortex-flame interaction, partial quenching within the highly turbulent separation zone close to the obstacle has been found to be a major reason for strong flame acceleration by highly blocking obstacles. Unburned radicals originating from aborted chemical reactions by turbulent separation of reacting molecules are "washed out" from the reaction zones to be carried with the accelerated jet flow and transported ahead of the flame, where they form a highly reactive mixture. When the disturbed flame front consisting of quite a number of small reacting shreds reforms behind the obstacle, it becomes intensely wrinkled and corrugated. Running into the radical-enriched region, the flame is strongly accelerated and local explosions would amplify themselves to detonation waves in DDT-sensitive mixtures.

NOMENCLATURE

δ_l	laminar flame thickness
ϕ	fuel equivalence ratio
γ_{H2}	H_2-concentration in vol.%
λ	heat conductivity
λ_T	Taylor micro scale of turbulence
ν	kinematic viscosity
ρ	density
τ_k	Kolmogorov micro time scale of turbulence
τ_L	integral time scale of turbulence
a	thermal diffusivity $a=\lambda/(\rho c_p)$
A_0	normal projection of the flame surface
A_{21}	quantum transfer coefficient
A_F	flame surface area
B_{12}	Einstein coefficient
BR	blockage ratio, ratio between blocked area and unblocked area
c_p	isobaric heat capacity
D	mass diffusivity

Da	Damköhler number
E_l	population of electronical ground state
$I_{v,L}$	spectral laser intensity
k	Kolmogorov micro scale of turbulence
K	Karlovitz flame stretch factor
Ka	Karlowitz number
L	integral length scale of turbulence
L_0	normal projection of the flame perimeter
Le	Lewis number, $Le = a/D$
L_F	flame perimeter
N	molecular number density
Pr	Prandtl number
Q_{2l}	quenching coefficient
Re_L	turbulent Reynolds number ref. to L
s_l	laminar burning velocity
s_T	turbulent burning velocity
u	mean flow velocity
u'	rms fluctuation velocity
u_F	flame propagation speed

ACKNOWLEDGMENTS

The work presented in this paper has been supported by the German Ministry of Education, Science, Research and Technology BMBF within the scope of the project no. 1500 824 [19].

REFERENCES

1. G. E. Andrews, D. Bradley, S. B. Lwakabamba, "Turbulence and Turbulent Flame Propagation - A Critical Appraisal", *Comb. and Flame*, Vol.24; (1975)
2. R. G. Abdel-Gayed, D. Bradley, M. Lawes, "Turbulent Burning Velocities: a General Correlation in Terms of Straining Rates", *Proc. R. Soc. Lond. A414*, pp. 389-413, (1987)
3. R. G. Abdel-Gayed, D. Bradley, F. K.-K. Lung, "Combustion Regimes and the Straining of Turbulent Premixed Flames", *Comb. and Flame*, Vol.76; (1989)
4. N. Brehm, F. Mayinger, "Limit for the Transition from Deflagration to Detonation in Hydrogen-/Air-/Steam-Mixtures", *final report BMBF no. 1500712*, (1988)
5. R. Borghi, "On the Structure of Turbulent Premixed Flames"; *Recent Advances in Aeronautical Science*, Eds.: C.Bruno, C.Casci; Pergamon Press; (1984)
6. M. Gonzalez, R. Borghi, A. Saouab, "Interaction of a Flame Front with Its Self-Generated Flow in an Enclosure: The 'Tulip Flame' Phenomenon", *Combustion and Flame*, Vol. 88, pp. 201-220, (1992)
7. A. Ü. A. Gorgeon, S. Gökalp, "A Planar Laser Induced Fluorescence Study of Turbulent Flame Kernel Groth and Fractal Characteristics", *Combustion Science and Technology*, Vol. 92, pp. 265-290, (1993)
8. P. J. Goix, I. G. Shepherd, "Lewis Number Effects on Turbulent Premixed Flame Structure", *Combustion Science and Technology*, Vol. 91, pp. 191-206, (1993)
9. R. K. Kumar, E. M. Bowles, "Flame Acceleration in Hydrogen/Air Mixtures in a Vertical Cylinder Filled with Obstacles", *Proc. of 2nd Intl. Conf. on Containment Design and Operation*, Toronto, (1990)
10. G. W. Koroll, R. K. Kumar, E. M. Bowles, "Burning Velocities of Hydrogen-Air Mixtures", *Comb. and Flame*, Vol.94; (1993)
11. R. K.Kumar, H. Tamm, "Flame Acceleration Effects on the Combustion of Hydrogen in Large Vessels", *Proc. of the Joint ASME/ANS Nucl. Eng. Conf., Portland*, Ore, (1984)
12. S. Kwon, L.-K. Tseng, G. M. Faeth, "Laminar Burning Velocities and Transition to Unstable Flames in $H_2/O_2/N_2$ and $C_3H_8/O_2/N_2$ Mixtures", *Combustion and Flame*, Vol. 90, pp. 230-246, (1992)
13. J. Laufer, "The Structure of Turbulence in Fully Developed Pipe Flow", *Rep. 1174, U.S. Nat. Adv. Com. Aero.*, (1954)
14. J. Loesel Sitar, C. K. Chan, A. Guerrero, F. Torchia, "Turbulent Burning Rates of Near Flammability-Limit H_2-Air-Steam Mixtures", *Proc. of 3rd. Intl. Workshop on Hydrogen Research for Reactor Safety, Sept. 19.-23., Munich*, (1994)
15. T.-W. Lee, J. G. Lee, D. A. Nye, D. A. Santavicca, "Local Response and Surface Properties of Premixed Flames During Interactions with Karman Vortex Streets", *Comb. and Flame*, Vol.94, (1993)
16. T.-W. Lee, G. L. North, D. A. Santavicca, "Surface Properties of Turbulent Premixed Propane/Air Flames at Various Lewis Numbers", *Combustion and Flame*, Vol. 93, pp. 445-456, (1993)
17. G. Markstein, "Nonsteady Flame Propagation", *AGARD-ograph No. 75*, pp. 97-102, Pergamon Press,Oxford, 1964
18. F. Mayinger, R. Beauvais, "Influence of the Flow Structure on the Propagation of Hydrogen-Air-Flames", *final report BMBF no. 1500 810*, (1994)
19. F. Mayinger, R. Beauvais, G. Strube, N. Ardey, "Influence of the Temperature on the Limits for the Transition from Deflagration to Detonation (DDT) in Hydrogen-/Air-/Steam-Mixtures", *final report BMBF no. 1500 824*, (1994)
20. N. Peters, "Laminar Flamelet Concepts in Turbulent Combustion", *21st. Symp. (Intl.) on Combustion*, The Combustion Institute; Pittsburgh; (1986)
21. H. Phylaktou, G. E. Andrews, "The Acceleration of Flame Propagation in a Tube by an Obstacle", *Combustion and Flame*, Vol. 85: pp 363-379, (1991)
22. D. D. Radford, C. K. Chan, D. P. McCooeye, R. S. Azad, "Initiation of Detonation by Flame-Vortex Interaction", *13th Intl. Coll. on Dynamics of Explosion and Reactive Systems*, Nagoya, (1991)
23. Wm. L. Roberts, J. F. Driscoll, M. C. Drake, J. W. Ratcliffe, "OH Fluorescence Images of the Quenching of a Premixed Flame During an Interaction with a Vortex", *24th. Symp. (Intl.) on Combustion/The Combustion Institute*, pp. 169-176, (1992)
24. R. Starke, P. Roth, "An Experimental Investigation of Flame Behavior During Explosions in Cylindrical Enclosures with Obstacles", *Combustion and Flame*, Vol. 75, pp 111-121, 1989
25. T. Takashi, H. Toshisuke, "Local Flame Front Disturbance Under Acceleration", *Combustion and Flame*, Vol. 84, pp. 66-72, (1991)